Bragg Gratings in Multimode and Few-Mode Optical Fibers

Toru Mizunami, *Member, OSA*, Tzvetanka V. Djambova, Tsutomu Niiho, and Sanjay Gupta

***Abstract*—Bragg gratings in optical fibers in multimode propagation are investigated experimentally and theoretically. Bragg gratings formed in optical fibers in multimode propagation show multiple reflection peaks or multiple transmission dips in the reflection or transmission spectra, respectively. For standard graded-index multimode fiber, the number of reflection peaks of a Bragg grating depends on excitation condition of propagating modes. The number of reflection peaks of a Bragg grating at around 1.55 μm is 19 for highly multimode excitation and 3–4 for lower order mode excitation. We analyze the phase-matching conditions of the propagating modes and identify half of the reflection peaks as the reflection to the same mode and the rest as the reflection to the neighboring modes. In dispersion-shifted fiber, a Bragg grating at around 0.8 μm in three-mode propagation shows three reflection peaks in the reflection spectrum. The temperature dependence of each reflection peak is similar to that of a conventional Bragg grating in single-mode fiber. Polarization dependence measured on a Bragg grating in multimode graded-index fiber is negligible. An advantage of Bragg gratings in multimode fiber (MMF) and the applications are discussed.**

***Index Terms*—Fiber Bragg grating (FBG), multimode fiber (MMF), optical fiber communication, polarization, principal mode, propagating mode.**

I. Introduction

FIBER Bragg gratings (FBG's) have been recognized as important fiber-optic devices used for spectral filtering, dispersion compensation, wavelength tuning, and sensing in optical communication and optoelectronics. Since the first demonstration by Meltz *et al.* [1], FBG's have been formed only in single-mode optical fibers, and the spectral characteristics have been well known [2]. However, single-mode fiber (SMF) has a small core diameter and therefore is not easy to couple with optical devices except SMF's or laser diodes. On the other hand, multimode fiber (MMF) has a merit of easy coupling with other light sources such as light-emitting diodes (LED's). Especially, graded-index MMF has relatively low dispersion and therefore is suitable for optical communication. If Bragg gratings in MMF's are possible and they have useful characteristics, it would contribute to new applications in optical communication and optoelectronics. Wasner *et al.* [3] calculated the reflection spectrum of a Bragg grating in MMF and proposed application to bending sensors. It was shown that a FBG near the cutoff wavelength had two reflection wavelengths [4]. Okude *et al.* [5] fabricated a Bragg grating in a short piece of MMF with a core diameter of 17.5 μm and spliced both ends with SMF's. As their FBG was excited with the fundamental mode only, the reflectivity exceeded 30 dB, and undesired coupling of the fundamental mode to the cladding modes [6] was suppressed. The present authors demonstrated formation of a Bragg grating in graded-index MMF and briefly reported the transmission spectrum [7]. However, detailed characteristics or analysis of a Bragg grating in MMF has not been reported.

In this paper, we report detailed spectral characteristics of Bragg gratings written in optical fibers in multimode propagation, including the temperature and polarization characteristics, present a theory of reflection of Bragg gratings in MMF, and discuss the mechanism of Bragg reflection. This paper in organized as follows. Section II presents the experiments of fabrication and measurement of Bragg gratings at a wavelength of 1.55 μm in standard graded-index MMF and those at a wavelength of 0.8 μm in dispersion shifted fiber (DSF). The transmission and reflection spectra are measured for different conditions of excitation of modes. The measurement on temperature dependence is also presented. In Section III, the analysis of the measured spectra and their temperature dependence is described. Polarization measurement is also performed, and the uniformity of index modulation in the core cross section is discussed on the basis of the result of the measured polarization dependence. Applications of multimode FBG's to bending sensors and laser tuning are also discussed in this section. Section IV contains the conclusion.

II. Experiment

A. Fabrication of Multimode Fiber Bragg Gratings

The experimental setup of Bragg-grating formation is shown in Fig. 1. We employed both the phase-mask method [8] and the two-beam interference method [1]. The ultraviolet light source was a narrowband KrF excimer laser [9]. The typical energy density per pulse was 0.27 J/cm^2 for the two-beam interference method and 0.07 J/cm^2 for the phase-mask method, respectively. The exposure length was 6 mm. The transmission or reflection spectra of the formed grating were measured with two different light sources: a halogen lamp and an edge-emitting LED with a SMF pigtail. These spectra were measured using an Ando AQ-6310B optical spectrum analyzer with a resolution of 0.1 nm.

Manuscript received July 6, 1999; revised Nov. 15, 1999. This study was supported in part by The Grant-in-Aid from the Ministry of Education, Science, Sports, and Culture.

T. Mizunami and T. V. Djambova are with the Department of Electrical Engineering, Faculty of Engineering, Kyushu Institute of Technology, Kitakysushu 804-8550, Japan (e-mail: mizunami@elcr.kyutcch.ae.jp).

T. Niiho is with Matsushita Electric Ind. Co., Osaka, Japan.

S. Gupta is with Ando Electric, Tokyo, Japan.

Publisher Item Identifier S 0733-8724(00)01318-9.

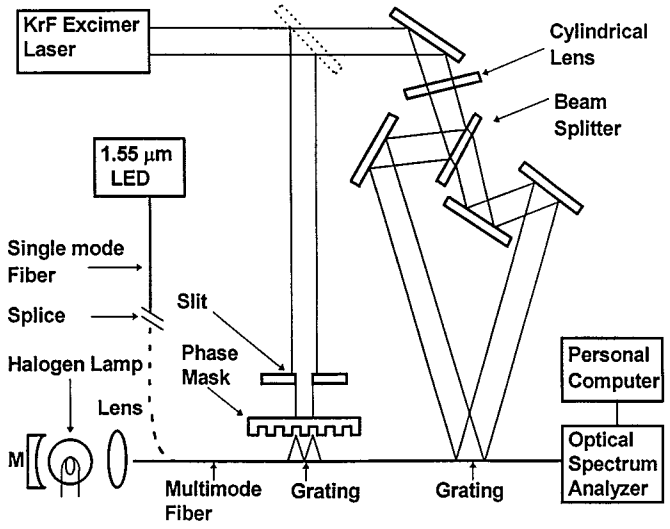

Fig. 1. Experimental setup for fabrication of multimode and few-mode fiber Bragg gratings.

We used graded-index MMF and DSF for fabrication of Bragg gratings. The MMF was standard graded-index fiber with a core diameter of 50 μm and a numerical aperture of 0.2. The DSF had a mode-field diameter of 8.2 μm and a numerical aperture of 0.2. We performed hydrogen loading on both fibers for 10–14 days at a pressure of 100 atm.

The observed spectra of a Bragg grating in MMF were very different for the two light sources. Fig. 2 shows a transmission spectrum obtained by an LED with a SMF pigtail. The Bragg grating in MMF was fabricated using the phase-mask method with an energy density of 0.07 J/cm^2, a repetition rate of 10 Hz, and an exposure time of 3 min. Four reflection wavelengths appeared, and the maximum reflectivity was 96.6% at 1559 nm. On the other hand, using a halogen lamp as a light source, the transmission spectrum of the same grating was measured as in Fig. 3. 19 dips (denoted "a"–"t") appeared, which corresponds to highly multimode excitation. The separation between these transmission dips is 0.8 nm, and the wavelength range of these dips is 16 nm. The maximum reflectivity is 36% at 1551.8 nm, and the total bandwidth defined by half of the maximum reflectivity is 10 nm full-width at half-maximum (FWHM). A reflection spectrum measured using a fiber coupler was the reverse of the transmission spectrum in Fig. 3. These results show that the measured spectra depend on the conditions of excitation of modes. Measurements using an LED with a SMF pigtail correspond to lower order mode excitation, and those using a halogen lamp correspond to highly multimode excitation. We applied index-matching oil on the surface of the Bragg grating shown in Fig. 3, but the reflection or transmission spectrum did not change. This means that these multiple transmission dips are not due to coupling to the cladding modes [6].

Fig. 4 shows the growth characteristics during fabrication of Bragg gratings in MMF comparing the two-beam interference method and the phase-mask method. The Bragg wavelengths of these FBG's were all about 1.55 μm. The reflectivity in Fig. 4 was measured with a SMF-pigtailed LED as a light source. For the phase-mask method at 50 Hz, a reflectivity of 90% was achieved within 40 s. For a repetition rate of 10 Hz, it took 200 s

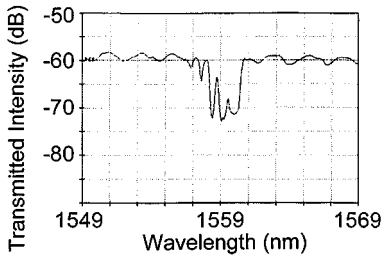

Fig. 2. Transmission spectrum of a Bragg grating in graded-index MMF for lower order mode excitation.

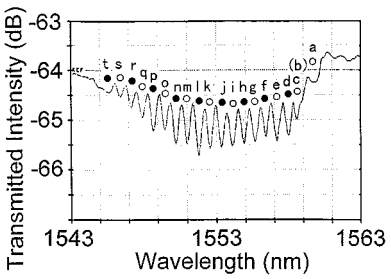

Fig. 3. Transmission spectrum of a Bragg grating in graded-index MMF for highly multimode excitation.

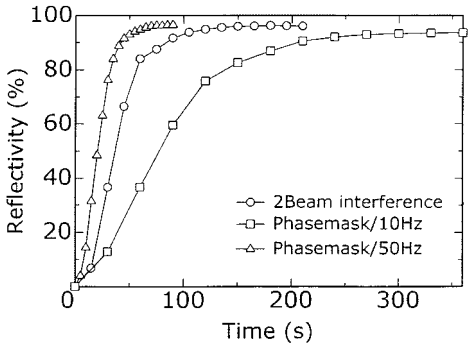

Fig. 4. Growth of reflectivity of Bragg gratings in graded-index multimode fiber for two-beam interference method at with repetition rate of 10 Hz (○), the phase mask method at 10 Hz (□) and the phase mask method at 50 Hz (△).

to reach 90% reflection. By the two-beam interference method at 10 Hz, the growth was more rapid than that by the phase-mask method at the same repetition rate. This is because the two-beam interference method was free from damage of a phase mask, and a higher energy density of 0.27 J/cm^2 was possible.

Next, Bragg gratings at 0.8 μm were fabricated in DSF using the two-beam interference method. A typical transmission spectrum measured using a halogen lamp as a light source is shown in Fig. 5. The energy density was 0.27 J/cm^2, the repetition rate was 10 Hz, and the irradiation time was 3 min. Three transmission dips (denoted "a"–"c") appeared. The separation between the transmission dips is 1.6 nm. The reflectivities were 35–50%.

B. Temperature Dependence

We measured the temperature dependence of each reflection wavelengths of a Bragg grating in MMF. For temperature measurements, the Bragg grating in MMF was placed on the Peltier heat pump, and the transmission spectrum was measured for the temperatures from -14.5 °C to $+132.5$ °C using a fiber coupler and a halogen lamp as a light source.

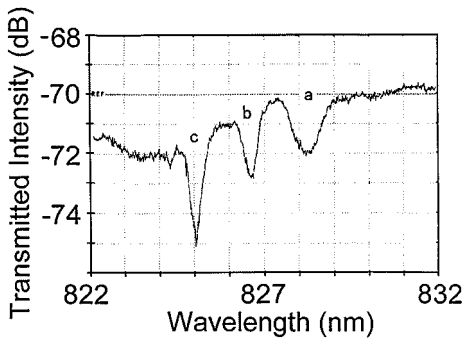

Fig. 5. Transmission spectrum of a few-mode FBG in dispersion shifted fiber.

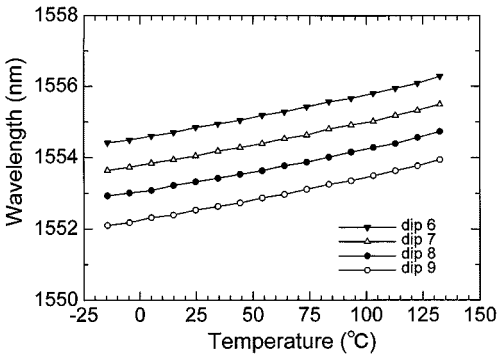

Fig. 6. Temperature dependence of reflection wavelengths of a Bragg grating in graded-index multimode fiber.

Fig. 6 shows measured results of wavelength shifts of four dips near the center of the spectrum as a function of temperature. The four dips of "6," "7," "8," and "9" in Fig. 6 correspond to "g," "h," "i," and "j" in Fig. 3, respectively, and the identification may include an error of plus/minus one dip. The solid lines in Fig. 6 show the best-fit linear curves. From this figure, we can obtain the temperature sensitivity of 11.5 pm/°C at room temperature or 12.5 pm/°C as an average from -14.5 °C to $+132.5$ °C.

III. Discussion

A. Analysis of Phase Matching Condition

The phase-matching condition, or Bragg reflection condition, of an index modulation with the period Λ is given by $\beta_1 - \beta_2 = 2\pi/\Lambda$, where β_1 and β_2 are the propagation constants of forward and backward propagating modes, respectively. For reflection to the same mode, $\beta_1 = -\beta_2 = \beta$. Then the phase-matching condition is simply $\beta = \pi/\Lambda$. For graded-index MMF, the number of propagating modes is usually calculated by the equation

$$M = \tfrac{1}{2}a^2k^2n_1^2\Delta \tag{1}$$

where

- a core radius;
- k wave number;
- n_1 refractive index of the core;
- Δ maximum relative index difference.

In the case of our MMF, the number of modes M is 103 at 1.55 μm. However, some of these modes have almost the same propagation constant. Therefore, we introduce the concept of principal mode: the modes having the same propagation constant is classified into the same principal mode [10],[11]. The propagation constant for the Nth principal mode is approximated by the equation

$$\beta = \frac{2\pi}{\lambda}n_1\sqrt{1 - 4\Delta\frac{N+1}{V}} \tag{2}$$

where

- V normalized frequency: $V = 2\pi aNA/\lambda$;
- NA numerical aperture.

The calculated propagation constants for our MMF are shown in Fig. 7. 10 principal modes are bound modes at around 1.55 μm. Open circles in Figs. 3 and 7 show the corresponding Bragg wavelengths in the experiment. Therefore, these ten Bragg wavelengths in the range from 1545 to 1560 nm are due to the reflection to the same mode. We also consider the reflection to the neighboring modes: reflection from the N mode to the $N+1$ mode and that from the $N+1$ mode to the N mode. In this case, we consider reflection of $\beta_1(>0)$ mode to $\beta_2(<0)$ mode. As the phase-matching condition is $\beta_1 + |\beta_2| = 2\pi/\Lambda$, the wavelength to be reflected is related to the average $\beta = (\beta_1 + |\beta_2|)/2$, which means the Bragg wavelength is in the middle of those of the N to N reflection and the $N+1$ to $N+1$ reflection. The experimental results agreed with these values are shown by black dots in Figs. 3 and 7. A theoretical reflection wavelength "b" was not observed in the experiment. Therefore, it was shown that the ten Bragg wavelengths were attributed to the reflection to the same mode, and the rest between them was attributed to the reflection to the neighboring modes.

Next, we discuss the measured spectrum of lower-order mode excitation in Fig. 2. In Fig. 2, the wavelength of the lowest- order mode ($N = 0$) reflection is 1560 nm. The wavelength of $N = 0$ reflection in Fig. 3 is also 1560 nm. The wavelength separations between the neighboring dips are 0.7 and 0.8 nm in Figs. 2 and 3, respectively. As these values agree well, the mechanism of reflection by a Bragg grating in MMF does not depend on the condition of excitation of modes.

On the other hand, for step-index multimode fiber, the relation between the normalized propagation constant b for the Nth principal mode for normalized frequency V is given by [10]

$$V = \sqrt{\frac{1}{1-b}}\left(\frac{N}{2}\pi + \frac{\pi}{4} + \tan^{-1}\sqrt{\frac{b}{1-b}}\right). \tag{3}$$

Using this equation, b can be calculated from N and V, and the propagation constant β is given by

$$\beta = \frac{2\pi}{\lambda}n_1\left[\left\{1 - (1-\Delta)^2\right\}b + (1-\Delta)^2\right]. \tag{4}$$

The calculated propagation constants for DSF and the Bragg wavelengths are shown in Fig. 8. Three propagating modes exist. The calculated Bragg wavelengths were 828.2, 826.9, and 824.9 nm for $N = 0, 1, 2$, respectively, for a writing angle of two laser beams of 26.5°. These wavelengths agree with those of experiment (828.3, 826.8, and 825 nm, respectively) in Fig. 5. The reflection to the neighboring modes did not appear in Fig. 5. This is considered to be because the difference in the

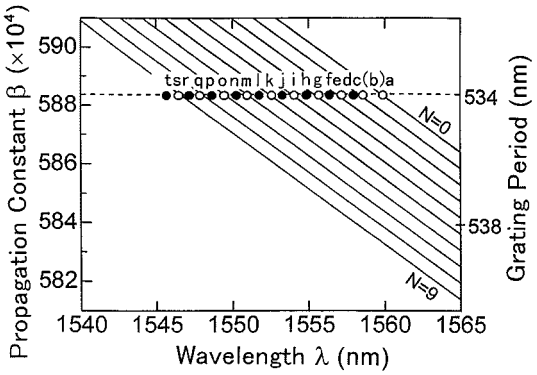

Fig. 7. Mode diagram of a Bragg grating in graded-index MMF. Lines show calculated propagation constants for a multimode graded-index fiber. Circles show the corresponding Bragg wavelength in Fig. 3. Open circles correspond to the reflection to the same mode, and filled circles correspond to the reflection to the neighboring mode.

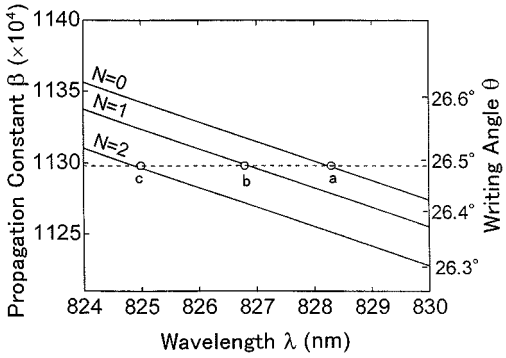

Fig. 8. Mode diagram of few-mode fiber Bragg grating. Lines show calculated propagation contants for dispersion-shifted fiber. Circles show the corresponding Bragg wavelengths in Fig. 5.

propagation constants is larger than that in graded-index MMF at 1.55 μm.

B. Temperature Dependence

We discuss the temperature dependence of reflection wavelengths of a Bragg grating in graded-index MMF. The temperature dependence of the Bragg wavelength is given by the differentiation of (2). For simplicity, we assume that the second term in the square root of (2) is much smaller than the unity and that the numerical aperture is approximated by $NA = n_1\sqrt{2\Delta}$, then the following equation is obtained:

$$\frac{d\lambda}{dT} = \frac{\lambda^2}{2n_1\Lambda^2}\frac{d\Lambda}{dT} + \left[\frac{\lambda^2}{2n_1^2\Lambda} - \frac{\lambda^2(N+1)(3n_2-2n_1)}{2\pi a n_1^2\sqrt{2n_1(n_1-n_2)}}\right]\frac{dn_1}{dT} + \frac{\lambda^2(N+1)}{2\pi a n_1\sqrt{2n_1(n_1-n_2)}}\frac{dn_2}{dT} \quad (5)$$

where n_2 is the refractive index of the cladding. dn_1/dT for GeO_2-doped silica core and dn_2/dT for silica cladding are almost the same value of 1×10^{-5}/°C at 589 nm [12]. As the thermal expansion coefficient $\alpha = (d\Lambda/dT)/\Lambda$ is a small value of 0.55×10^{-6} [1], [13], the first term in (5) is one order less than the second term. At 1.55 μm, the terms having N increase $d\lambda_N/dT$ by 1.3% for maximum N, if dn_1/dT and dn_2/dT are equal. According to a recent measurement on long-period fiber gratings [14], dn_1/dT for a GeO_2 concentration of 10 mol% is larger than dn_2/dT by 6×10^{-7}, then the terms having N decrease $d\lambda_N/dT$ by 1.5% for maximum N. As these values are small, the reflection peaks have almost the same temperature dependence of 11.4 pm/°C for all N. This is the same for reflection to the neighboring modes. This result agrees with the measured temperature sensitivity of 11.5 pm/°C at room temperature in Fig. 6. In addition, the spectral profile did not change with the temperature. If the temperature distribution along the Bragg grating is controlled [15], the spectral profile will change.

C. Polarization Dependence of a Multimode Fiber Bragg Grating

As the core diameter of the MMF is a large value of 50 μm, ultraviolet writing beam may not be uniform over the core cross section due to attenuation by absorption. To study this uniformity, we measured the polarization dependence of a Bragg grating in MMF. Fig. 9 presents three possible models of FBG's. The reflectivity of a conventional axially symmetric grating [Fig. 9(a)] does not depend on the polarization. It has been known that the reflection from a type II grating [16]–[18] [Fig. 9(b)] is strongly polarization dependent [18]. The damage tracks localized on one side of the core [16], [17] are responsible for this polarization sensibility. The axially asymmetric grating [Fig. 9(c)] is considered to be weakly polarization dependent.

We measured the polarization of the reflected light from a Bragg grating in MMF using a setup shown in Fig. 10. Amplified spontaneous emission from an erbium-doped fiber pumped with a 1.48-μm laser diode was used as a nonpolarized light source. The amplified spontaneous emission was introduced through a fiber coupler with a branching ratio of 50 : 50 into the MMF with a Bragg grating. The reflected light was introduced into a halfwave polarization controller and filtered with a polarization dependent isolator. The light with a specific polarization was measured with an optical spectrum analyzer. The Bragg grating used for the measurement was made in MMF using the phase-mask method with a 0.534-μm periodicity and a 6-mm length. Therefore, the fibers in the measurement system were all SMF's except that the MMF with a Bragg grating was spliced with a port of the coupler.

Fig. 11 shows the dependence of the reflectivity on the angle of polarization. The measured variation in the reflected power is less than 1 dB, which is within the error of the measurement. From this result, we consider that the grating in the present experiment is axially uniform grating, and the refractive index change is considered to be uniform over the core cross section.

D. Applications

As MMF has a large core diameter of typically 50 or 62.5 μm, it is easy to couple with other lasers or optical sources. A solid state laser is difficult to couple with SMF, and therefore it can be a candidate to be tuned with a Bragg grating in MMF. We

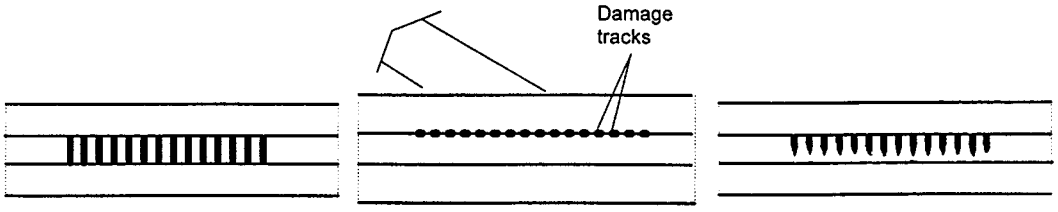

Fig. 9. Models of various fiber Bragg gratings and their polarization dependence: (a) axially symmetric grating with no polarization dependence, (b) type II grating with strong polarization dependence, and (c) axially asymmetric grating with weak polarization dependence.

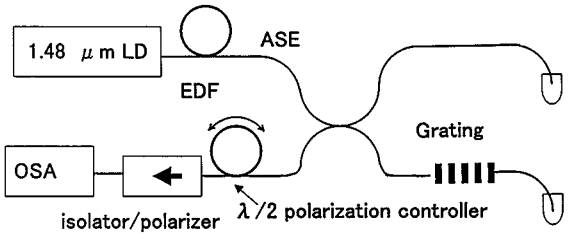

Fig. 10. Experimental setup for polarization measurement of a Bragg grating in graded-index MMF.

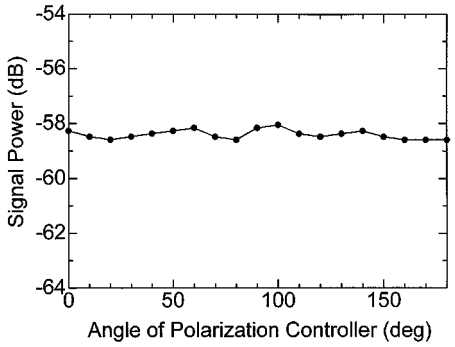

Fig. 11. Measured result of polarization dependence of a Bragg grating in graded-index MMF.

fabricated a Bragg grating at 0.84 μm in MMF, and it was used for tuning of a $Cr^{3+}:LiSrAlF_6$ laser [19]. The spectral width decreased from 7 to 2.5 nm by using a Bragg grating in MMF, although single-longitudinal-mode operation was achieved only by a Bragg grating in SMF. This technique may be applied to other solid-state lasers such as $Ti^{3+}:Al_2O_3$ lasers. Another laser tuned with a Bragg grating in MMF will be a semiconductor laser. Especially, a vertical-cavity surface-emitting laser (VCSEL) for optical communication has a large emitting area and therefore is suitable for coupling with MMF. Fig. 12(a) shows the concept of a MMF communication system using a VCSEL tuned with a Bragg grating in MMF. As a preliminary experiment, we demonstrated the decrease in the spectral width to 1/2–1/3 from the initial values. The details of the experiment will be reported elsewhere. It will also be possible to reduce the number of propagating modes in MMF and thus to reduce the modal dispersion in communication, because mode selection will occur in laser oscillation.

The sensing applications were proposed by Wanser *et al.*[3]. When MMF with a Bragg grating is bent, the reflection and transmission spectra change. In our experiment, the reflectivity of the lower order mode increases and that of the higher order mode decreases when the fiber is bent. This is almost consistent with the calculation by Wanser *et al.* [3]. In our measurement, the bending dependence of DSF with a Bragg grating was similar. A Bragg grating in DSF has a simple spectral structure of only three reflection wavelengths as shown in Fig. 5. Also, a Bragg grating in DSF had a higher sensitivity to bending. Some of the other characteristics of bending sensors are reported in [20]. A practical bending sensor can be constructed as shown in Fig. 12(b). In this sensor, transmission or reflection spectrum is observed using a tunable source, and then bending is given on the MMF having a Bragg grating. The tunable source can be replaced by a combination of a broadband source and a tunable filter. Also, a displacement sensor as shown in Fig. 12(c) is possible, where the displacement is translated into bending using a deformer, and interrogation is the same with that in Fig. 12(b).

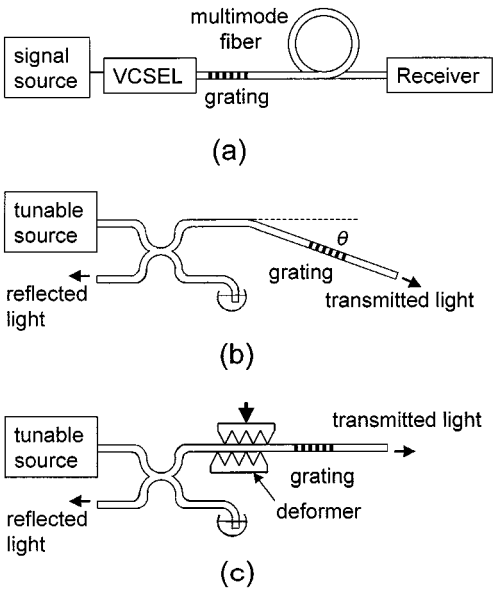

Fig. 12. Concept of application of multimode or few-mode fiber Bragg gratings: (a) multimode-fiber communication system using a vertical-cavity surface-emitting laser (VCSEL) coupled with a multimode fiber Bragg grating, (b) fiber-optic bending sensor to detect the bending angle θ, and (c) fiber-optic displacement sensor using bending dependence of a multimode or few-mode fiber Bragg grating.

IV. Conclusion

We fabricated Bragg gratings in graded-index MMF and in DSF, and measured their reflection and transmission characteristics. For lower order mode excitation by coupling with an LED

through a SMF pigtail, the Bragg grating in MMF at around 1.55 μm had four reflection wavelengths, and the reflectivity was as high as 96.6%. In contrast, for highly multimode excitation using a halogen lamp, the same FBG showed 19 reflection wavelengths in the reflection spectrum. We performed an analysis on the phase-matching condition, and attributed the ten reflection wavelengths to the reflection to the same mode, and attributed the rest to the reflection to the neighboring modes. The Bragg wavelengths of the fundamental principal mode on the two different excitation conditions agreed with each other. A Bragg grating at 0.8 μm in DSF had three Bragg wavelengths. These wavelengths also agreed with the mode analysis. However, reflection to the neighboring modes did not appear, because the difference in the propagation constants is large. The temperature dependence of each reflection peak of a Bragg grating in MMF agreed with the analysis. We also performed a polarization measurement of a Bragg grating in MMF, and concluded that the index modulation is sufficiently uniform in the core cross section. Bragg gratings in MMF will be useful for spectral control of a laser having a relatively large beam diameter and difficult to couple with SMF. Bragg gratings in multimode or few-mode fibers can be used for bending or displacement sensors.

ACKNOWLEDGMENT

The authors would like to thank T. Yamao for technical assistance in the experiment.

REFERENCES

[1] G. Meltz, W. W. Morey, and W. H. Glenn, "Formation of Bragg gratings in optical fibers by a transverse holographic method," *Opt. Lett.*, vol. 14, pp. 823–825, Aug. 1989.

[2] A. Othonos, "Fiber Bragg gratings," *Rev. Sci. Instrum.*, vol. 68, pp. 4309–4341, Dec. 1997.

[3] K. H. Wanser, K. F. Voss, and A. D. Kersey, "Novel fiber devices and sensors based on multimode fiber Bragg gratings," *Proc. SPIE*, vol. 2360, pp. 265–268, 1994.

[4] W. W. Morey, G. Meltz, J. D. Love, and S. J. Hewlett, "Mode-coupling characteristics of UV-written Bragg gratings in depressed-cladding fiber," *Electron. Lett.*, vol. 30, pp. 730–732, Apr. 1994.

[5] S. Okude, M. Sudoh, K. Shima, T. Sakai, A. Wada, and R. Yamauchi, "A novel technique for suppressing undesired coupling of LP_{01} mode to cladding modes in fiber Bragg grating," in *Tech. Dig., 11th Int. Conf. Optical Fiber Sensors*, Sapporo, Japan, May 1996, pp. 380–383.

[6] V. Mizrahi and J. E. Sipe, "Optical properties of photosensitive fiber phase gratings," *J. Lightwave Technol.*, vol. 11, pp. 1513–1517, Oct. 1993.

[7] T. Mizunami, S. Gupta, T. Yamao, and T. Shimomura, "Multimode fiber Bragg gratings-spectral characteristics and applications," in *Int. Conf. Integrated Optics Optical Fiber Commun./Eur. Conf. Optical Commun.*, vol. 3, Sept. 1997, pp. 182–185.

[8] K. O. Hill, B. Malo, F. Bilodeau, D. C. Johnson, and J. Albert, "Bragg gratings fabricated in monomode photosensitive optical fiber by UV exposure through a phase mask," *Appl. Phys. Lett.*, vol. 62, pp. 1035–1037, Mar. 1993.

[9] T. Mizunami, S. Gupta, and T. Shimomura, "KrF-laser induced fiber Bragg gratings: Formation characteristics and cutback measurement," *Japan. J. Appl. Phys.*, pt. 1, vol. 35, pp. 4349–4352, Aug. 1996.

[10] Y. Suematsu and K. Iga, *Hikari Faiba Tsuusin Nyuumon* (in Japanese), 3rd ed. Tokyo, Japan: Ohmusha, 1989, p. 184, 188, 189, and 194.

[11] K. Kitayama, S. Seikai, and N. Uchida, "Impulse response prediction based on experimental mode coupling coefficient in a 10-km long graded-index fiber," *IEEE J. Quantum Electron.*, vol. QE-16, pp. 356–362, Mar. 1980.

[12] S. Takahashi and S. Shibata, "Thermal variation of attenuation for optical fibers," *J. Non-Cryst. Solids*, vol. 30, pp. 359–370, 1979.

[13] G. Meltz and W. W. Morey, "Bragg grating formation and germanosilicate fiber photosensitivity," *Proc. SPIE*, vol. 1516, pp. 185–199, 1992.

[14] Y. G. Han, C. S. Kim, K. Oh, U. C. Paek, and Y. Chung, "Performance enhancement of strain and temperature sensors using long period fiber grating," in *Proc. SPIE Int. Conf. Optical Fiber Sensors*, vol. 3746, Apr. 1999, pp. 58–61.

[15] S. Gupta, T. Mizunami, and T. Shimomura, "Computer control of fiber Bragg grating spectral characteristics using a thermal head," *J. Lightwave Technol.*, vol. 15, pp. 1925–1928, Oct. 1997.

[16] J. L. Archambault, L. Reekie, and P. St. J. Russell, "100% reflectivity Bragg reflectors produced in optical fibers by a single excimer laser pulses," *Electron. Lett.*, vol. 29, pp. 453–455, Mar. 1993.

[17] B. Malo, D. C. Johnson, F. Bilodeau, J. Albert, and K. O. Hill, "Single-excimer-pulse writing of fiber gratings by use of a zero-order nulled phase mask: Grating spectral response and visualization of index perturbations," *Opt. Lett.*, vol. 18, pp. 1277–1279, Aug. 1993.

[18] C. G. Askins, M. A. Putnam, G. M. Williams, and E. J. Friebele, "Contiguous fiber Bragg grating arrays produced on-line during fiber draw," *Proc. SPIE*, vol. 2191, pp. 80–85, 1994.

[19] N. J. Vasa, P. Husayin, M. Kidosaki, T. Okada, M. Maeda, and T. Mizunami, "Fiber grating butt-coupled cw $Cr^{3+}:LiSrAlF_6$ laser performance," in *Tech. Dig. Conf. Lasers and Electro-Optics*, San Francisco, CA, May 1998, pp. 67–68.

[20] T. Mizunami, T. Niiho, and T. V. Djambova, "Multimode fiber Bragg gratings for fiber optic bending sensors," *Proc. SPIE*, vol. 3746, pp. 216–219, Apr. 1999.

Toru Mizunami received the B.E., M.E., and Dr. E. degrees in electrical engineering from Kyushu University, Fukuoka, Japan, 1978, 1980, and 1984, respectively.

From 1984 to 1988, he was a Research Associate with the Electronics Department, Kyushu Institute of Technology, Kitakyushu, Japan. In 1988, he was appointed a Lecturer with the Electrical Engineering Department. Since 1989, he has been an Associate Professor with the Electrical Engineering Department. His main fields of interest are fiber Bragg gratings, nonlinear optics in fibers, fiber lasers, and excimer-laser processing.

Dr. Mizunami is a member of the Optical Society of America (OSA), the Institution of Electrical, Information and Communication Engineers (IEICE) of Japan, the Institution of Electrical Engineers of Japan, the Japan Society of Applied Physics, and the Laser Society of Japan.

Tzvetanka V. Djambova received the M.Sc. degree in physics from Plovdiv University, Plovdiv, Bulgaria, in 1985 and the Ph.D. degree in electronics from Université de Bretagne Occidentale, Brest, France in 1994.

In 1997, she joined the Institute of the Applied Physics, Technical University of Sofia, Bulgaria, as an Assistant Professor. Since 1998, she has been a Postdoctoral Fellow at Kyushu Institute of Technology, Japan, under the JSPS program. Her current research interests are fiber Bragg gratings, applications in optical fiber sensors, and optical communication.

Tsutomu Niiho, photograph and biography not available at the time of publication.

Sanjay Gupta was born in New Delhi, India, in 1965. He received the M.Tech. degree in optoelectronics and optical communication from the Indian Institute of Technology, Delhi, in December 1989. In 1998, he received the Dr.E. degree in electrical engineering from Kyushu Institute of Technology, Kitakyushu, Japan.

In 1998, he joined Ando Electric Co., where he has been engaged in research on fiber-optic and electrooptic sensors.